

$pp \rightarrow A \rightarrow Zh$ and the wrong-sign limit of the Two-Higgs-Doublet Model

Pedro M. Ferreira^{a,b}, Stefan Liebler^c, Jonas Wittbrodt^d

^a*Instituto Superior de Engenharia de Lisboa - ISEL, 1959-007 Lisboa, Portugal*

^b*Centro de Física Teórica e Computacional, Universidade de Lisboa, 1649-003 Lisboa, Portugal*

^c*Institute for Theoretical Physics, Karlsruhe Institute of Technology, 76131 Karlsruhe, Germany*

^d*DESY, Notkestraße 85, 22607 Hamburg, Germany*

Abstract

We point out the importance of the decay channels $A \rightarrow Zh$ and $H \rightarrow VV$ in the wrong-sign limit of the Two-Higgs-Doublet Model (2HDM) of type II. They can be the dominant decay modes at moderate values of $\tan\beta$, even if the (pseudo)scalar mass is above the threshold where the decay into a pair of top quarks is kinematically open. Accordingly, large cross sections $pp \rightarrow A \rightarrow Zh$ and $pp \rightarrow H \rightarrow VV$ are obtained and currently probed by the LHC experiments, yielding conclusive statements about the remaining parameter space of the wrong-sign limit. In addition, mild excesses – as recently found in the ATLAS analysis $b\bar{b} \rightarrow A \rightarrow Zh$ – could be explained. The wrong-sign limit makes other important testable predictions for the light Higgs boson couplings.

1 Introduction

After the discovery of a Standard Model (SM)-like Higgs boson with a mass of 125 GeV at the LHC [1, 2] the experimental collaborations put a large effort on the precise determination of its mass [3] and its couplings to the other SM fermions and gauge bosons [4]. Even though no significant deviations from the SM predictions were observed, there is plenty of room for the SM-like Higgs boson to be part of an extended Higgs sector. Accordingly, apart from the precise determination of the SM-like Higgs boson's properties, the search for additional Higgs bosons is ongoing. A well-motivated, simple extension of the SM Higgs sector is the class of Two-Higgs-Doublet Models (2HDMs), which were introduced by Lee in 1973 [5] to explain the observed matter-antimatter asymmetry as arising from a spontaneous breaking of \mathcal{CP} . The field content of the SM is complemented with an extra $SU(2)$ doublet, which even in the \mathcal{CP} -conserving case results in a richer scalar spectrum: two \mathcal{CP} -even scalars, the lightest h and the heavier Higgs boson H , a pseudoscalar A and two charged scalars H^\pm . In the 2HDM a softly broken \mathbb{Z}_2 symmetry is commonly extended to the Yukawa sector to prevent the appearance of tree-level flavor changing neutral currents [6, 7]. This procedure results in four distinct 2HDM

Electronic addresses: pmmferreira@fc.ul.pt, stefan.liebler@kit.edu, jonas.wittbrodt@desy.de.

types, some of which include a peculiar and interesting region of parameter space called the wrong-sign limit [8–14]. In this region, there is a relative sign between the couplings of the SM-like Higgs boson to down-type quarks and to gauge bosons with far-reaching phenomenological consequences. This sign change – the down-type quark couplings to the SM-like Higgs boson in the 2HDM acquire the opposite sign as in the SM – is a physical quantity, as it has physical consequences which cannot be removed by some field redefinition.

Standard searches for additional Higgs bosons focus on the decays into fermions and gauge bosons. In particular in some 2HDM types, where the coupling to down-type fermions is enhanced through large values of $\tan\beta$, searches in the $\tau^+\tau^-$ final state [15,16] are very powerful in setting limits on the 2HDM parameter space. On the other hand, for low values of $\tan\beta$, the 2HDM parameter space is probed by heavy Higgs decays into a pair of top quarks [17] or gauge bosons [18–25]. Searches in the di-photon channel are especially useful to constrain pseudoscalars below $m_A < 350$ GeV [26,27]. Since the discovery of a light Higgs h at 125 GeV the search for pseudoscalars decaying into a gauge boson Z and the light Higgs h has been deserving special attention and was carried out at 8 TeV [28,29] and 13 TeV [30,31]. If the mass splitting between the pseudoscalar and the heavy \mathcal{CP} -even Higgs boson is large enough, also $H \rightarrow ZA$ and $A \rightarrow HZ$ constrain parts of the parameter space [32,33]. Lastly, \mathcal{CP} -even Higgs decays into a pair of light Higgs bosons probe corners of the parameter space [34–41]. Ref. [42] provides a recent overview of excluded parameter regions from the various mentioned decays in the 2HDM. In this paper, we emphasize that in the wrong-sign limit of the 2HDM of types II/F both $A \rightarrow Zh$ and $H \rightarrow VV$ can be dominant, even if the decay into a pair of top quarks is kinematically open. Therefore the small deviation in the search $b\bar{b} \rightarrow A \rightarrow Zh$ with $h \rightarrow b\bar{b}$ at masses of the pseudoscalar around ~ 440 GeV observed by the ATLAS collaboration, see Ref. [31], with $0.1 - 0.3$ pb above the SM background, can be explained in the wrong-sign limit. The search assumed leptonic decays of the Z boson as hadronic decays of the Z boson only become useful at higher invariant masses of the pseudoscalar [43]. We note that the region of interest was also probed by the 8 TeV ATLAS and CMS analysis [28,29], which already set bounds on cross sections of similar size. The initial 13 TeV analysis [30] carried out by the ATLAS collaboration with an integrated luminosity of 3.2fb^{-1} also shows upward fluctuations, though at larger cross sections. If the small excess is confirmed, a signal in the gluon-fusion induced production mode is likely to be seen as well, at least at intermediate values of $5 < \tan\beta < 7.5$. On the other hand, if not confirmed, the upcoming data accumulated in the searches for heavy Higgs bosons, both in $A \rightarrow Zh$ and $H \rightarrow VV$, will conclusively probe the remaining parameter space of the wrong-sign limit. In contrast, the decay of the \mathcal{CP} -even Higgs boson into two light SM-like Higgs bosons is not yet sensitive to the parameter region under discussion.

The wrong-sign limit also makes testable predictions for the light Higgs boson couplings, most prominently it enhances the gluon-fusion cross section and simultaneously reduces the partial width into two photons. These deviations from the SM Higgs properties of the light Higgs boson do not decouple and therefore also limit the parameter space of the wrong-sign limit. We base our numerical analysis on a data set that does not only take into account the light Higgs boson data and the searches for heavy Higgs bosons, but also theoretical considerations like boundedness from below, stability and perturbativity of the scalar potential. It also respects

bounds from B -physics and electroweak precision measurements.

Our paper is organized as follows: In Section 2 we provide an introduction to the Two-Higgs-Doublet Model including the four different types and define the wrong-sign limit. Based on an extensive data set generated for the 2HDM of type II, Section 3 explains the enhancement of $pp \rightarrow A \rightarrow Zh$ in the wrong-sign limit. We discuss other phenomenological consequences of the wrong-sign limit in Section 4. In particular, we address the enhancement of $pp \rightarrow H \rightarrow VV$, which is also under current experimental investigation and present the deviations in the light Higgs boson signal strengths induced by the wrong-sign limit. We conclude in Section 5.

2 The 2HDM and the wrong-sign limit

As we argued in the introduction, the Two-Higgs-Doublet Model (2HDM) is one of the simplest extensions of the SM Higgs sector. Despite its simplicity, the model boasts a rich phenomenology. Spontaneous \mathcal{CP} breaking is possible, some versions of the model provide natural candidates for dark matter or tree-level flavor changing neutral currents (FCNC) whose magnitude can be made naturally small via appropriate symmetries (for a recent review, see [44]). In the most used versions of the model, a global \mathbb{Z}_2 symmetry is imposed on the Lagrangian, softly broken by a dimension two term. This symmetry is introduced to eliminate tree-level flavor changing neutral currents in the Yukawa sector [6, 7]. The scalar potential for this version of the model may be written as

$$V = m_{11}^2 |\Phi_1|^2 + m_{22}^2 |\Phi_2|^2 + m_{12}^2 \left[\Phi_1^\dagger \Phi_2 + \text{h.c.} \right] \\ + \frac{\lambda_1}{2} |\Phi_1|^4 + \frac{\lambda_2}{2} |\Phi_2|^4 + \lambda_3 |\Phi_1|^2 |\Phi_2|^2 + \lambda_4 |\Phi_1^\dagger \Phi_2|^2 + \frac{\lambda_5}{2} \left[\left(\Phi_1^\dagger \Phi_2 \right)^2 + \text{h.c.} \right], \quad (1)$$

with all 8 parameters real. The quartic couplings of the model must obey well-known bounded from below conditions [45–48] and other constraints to ensure perturbative unitarity [49, 50].

After spontaneous symmetry breaking the doublets Φ_1 and Φ_2 acquire real vacuum expectation values (vevs), v_1 and v_2 . To ensure that the electroweak gauge bosons have their known masses the relation $v_1^2 + v_2^2 = v^2$ with $v = 246$ GeV, has to hold. The model’s scalar sector is usually described in terms of the following set of parameters: the vev v ; the four physical scalar masses (those of h , H , A and H^\pm); the angle β , defined such that $\tan \beta = v_2/v_1$; the angle α , which is the diagonalization angle for the (2×2) \mathcal{CP} -even mass matrix; and the soft-breaking term in the scalar potential, m_{12}^2 . Without loss of generality, we may take the interval of variation of α to be $-\pi/2 \leq \alpha \leq \pi/2$. Notice both possible signs for this parameter. In all that follows, we will assume that the light \mathcal{CP} -even Higgs boson h is the one that has been observed at the LHC. Thus we fix $m_h = 125$ GeV.

As for the Yukawa sector, it can be shown that for the \mathbb{Z}_2 symmetry to eliminate tree-level FCNC, each set of same-charge fermions should couple to a single scalar doublet. This leaves four possibilities for the scalar-fermion couplings, summarized in Tab. 1. In what regards the quark sector, models I and Lepton Specific (LS) have almost identical phenomenologies,

	u -type	d -type	leptons
Type I	Φ_2	Φ_2	Φ_2
Type II	Φ_2	Φ_1	Φ_1
Lepton Specific (LS)	Φ_2	Φ_2	Φ_1
Flipped (F)	Φ_2	Φ_1	Φ_2

Table 1: Couplings between fermion and Higgs doublets in the four Yukawa types of the softly broken \mathbb{Z}_2 -symmetric 2HDM.

as do models II and Flipped (F). There are significant constraints on the models' parameter space, stemming from B -physics, in particular from $b \rightarrow s\gamma$ measurements [51–55]. Roughly, these constraints translate into a lower bound on $\tan\beta$ (we will take $1 \leq \tan\beta \leq 35$) and, for Model II and the Flipped model, a lower bound on the mass of the charged scalar (we will take $m_{H^\pm} \geq 480$ GeV). Please notice that the latest results from Ref. [55] already put this bound at about 580 GeV, a point to which we shall return.

The mixing between the two Higgs doublet alters the couplings of h *vis a vis* what one would expect if the lightest \mathcal{CP} -even was exactly the SM Higgs. It is customary to define

$$\kappa_X^2 = \frac{\Gamma^{\text{2HDM}}(h \rightarrow X)}{\Gamma^{\text{SM}}(h \rightarrow X)} \quad (2)$$

for each SM decay state X . At tree-level, this ratio is simply the square of the ratio of the couplings $\kappa_X = g_X^{\text{2HDM}}/g_X^{\text{SM}}$. For the ZZ and WW couplings to h , one obtains

$$\kappa_{VV} = \sin(\beta - \alpha) \quad (3)$$

for all 2HDM model types. Given the ranges allowed for both α and β and LHC results indicating SM-like behavior for h , one finds that $\kappa_{VV} > 0$, so the coupling of h to the electroweak gauge bosons in the 2HDM always has the same sign as in the SM. As for the couplings of h to up-type quarks, they are such that

$$\kappa_U = \frac{\cos\alpha}{\sin\beta} \quad (4)$$

for all Yukawa models, since Φ_2 always couples to up-type quarks. For down-type quarks, one has for models I and LS

$$\kappa_D = \frac{\cos\alpha}{\sin\beta} \quad (5)$$

and for models II and F,

$$\kappa_D = -\frac{\sin\alpha}{\cos\beta}. \quad (6)$$

Given that $\tan\beta > 0$ and the angle α ranges from $-\pi/2$ to $\pi/2$, it is easy to see that $\kappa_U > 0$. However, though for models I and LS $\kappa_D > 0$, for models II and F that is no longer true — the

coupling of the light Higgs boson h to down-type quarks in the 2HDM of type II/F can have the opposite sign to the respective SM coupling and to κ_{VV} . This *wrong-sign limit* [8–14] is realized if $\alpha > 0$. More useful information can be gathered if one rewrites Eq. (5) as

$$\kappa_D = -\frac{\sin \alpha}{\cos \beta} = \sin(\beta - \alpha) - \cos(\beta - \alpha) \tan \beta. \quad (7)$$

Since the light Higgs boson h should behave like the SM Higgs boson [4] one must have $\sin(\beta - \alpha) \simeq 1$. Thus the only possibility to have a negative sign in κ_D is if $\cos(\beta - \alpha) \tan \beta \simeq 2$, which points to higher values of $\tan \beta$ and $\cos(\beta - \alpha) > 0$. In fact, current LHC results still allow for sizeable values of $\cos(\beta - \alpha)$ ($\sim 0.3 - 0.4$).

The wrong-sign limit is not merely a strange corner of parameter space. It has, in fact, phenomenological consequences observable at the LHC. The change in sign of the bottom-quark coupling affects both the gluon-fusion production cross section – enhancing it – and the di-photon branching ratio of the light Higgs boson h – suppressing it.¹ As a consequence, the wrong-sign limit is an example of a nondecoupling regime within the 2HDM, as it cannot lead to light Higgs boson properties exactly equal to ones of the SM Higgs boson [8], a point which we will address again in Section 4. We note that the wrong-sign limit is also under tension from requesting validity of the model up to just a few TeV [56]. We will now consider the effect of the wrong-sign limit on other observables, in particular the production of a pseudoscalar and its subsequent decay to Zh . In the 2HDM of type II the couplings $A - Z - h$ and $H - V - V$ are proportional to $\cos(\beta - \alpha)$ and therefore lead to sensitivity to the wrong-sign limit in searches for heavy scalars in Zh and VV final states. Lastly, the coupling $H - h - h$ also increases with $\cos(\beta - \alpha)$ yielding a potential sensitivity in future di-Higgs searches.

3 $pp \rightarrow A \rightarrow Zh$ in the wrong-sign limit

Recently, in Ref. [31], the ATLAS collaboration reported a small deviation on the search channel $pp \rightarrow A \rightarrow Zh$: an excess, relative to background expectations, of $0.1 - 0.3$ pb for $\sigma(pp \rightarrow A \rightarrow Zh)\text{BR}(h \rightarrow b\bar{b})$, for a potential pseudoscalar mass of about 440 GeV. The significance is larger in case the pseudoscalar A is produced through bottom-quark annihilation rather than gluon fusion, but both production processes show a deviation. The statistical significance of this excess is (yet) too low to indicate anything meaningful, but it does raise the question: would it be possible to account for such an excess within the framework of the 2HDM? Common wisdom suggests that for that mass range both the production cross sections and the branching ratios into Zh would be too small for an excess to occur. In fact, for such masses, one is above the $t\bar{t}$

¹The enhancement of the gluon fusion cross section can be understood by expanding it in terms of the dominant top- and bottom-quark amplitudes, A_t and A_b . The cross section is proportional to $|A_t + A_b|^2 = |A_t|^2 + \text{Re}(A_t A_b) + |A_b|^2$. The second term changes sign upon flipping the sign of the bottom-quark Yukawa coupling. Since this term is negative in the SM this leads to an enhancement of the cross section in the wrong-sign limit (see also footnote 3). A similar argument holds for the di-photon branching ratio with additional W boson and charged Higgs boson in the loop, where the effect of the negative bottom quark Yukawa is however much less pronounced. The dominant negative interference for the di-photon branching ratio is induced through the additional charged Higgs boson, see the discussion of Fig. 6.

threshold and the cross section for gluon fusion is expected to decrease rapidly. Furthermore, since the pseudoscalar can decay to a pair of top quarks, that decay channel would be expected to dominate over all others.

However, several details of the 2HDM allow to overcome those initial difficulties. To wit:

- The gluon-fusion production cross section is expected to be larger for a pseudoscalar A (of a 2HDM with $\tan\beta = 1$) than for a SM scalar H . At leading order, both processes occur due to a triangle fermion loop diagram. To illustrate the enhancement for a pseudoscalar, we compare the top-triangle contribution to the production cross section for a pseudoscalar mass of $m_A = 440$ GeV with the analogous contribution for a scalar of the same mass. We conclude that the pseudoscalar cross section is $|a_q^A(x_A)/a_q^H(x_H)|^2 \simeq 2.36$ times larger than the scalar cross section, with $x_\phi = m_\phi^2/4m_t^2$. The functions a_q^ϕ can e.g. be found in Ref. [57]. The ratio is also hardly affected by higher-order contributions. At next-to-next-to-leading order (NNLO) QCD [58–62] it yields $\sigma(gg \rightarrow A)/\sigma(gg \rightarrow H) = 17.03 \text{ pb}/7.16 \text{ pb} \sim 2.38$ at a center-of-mass energy of 13 TeV even including bottom- and charm-quark effects at next-to-leading (NLO) QCD [63]. The numbers are produced with `SusHi 1.6.0` [57, 64].
- In the 2HDM of type II, the coupling of the pseudoscalar to the top quark is proportional to $1/\tan\beta$, but the coupling to bottom quarks grows with $\tan\beta$. Therefore, with increasing $\tan\beta$ bottom-quark annihilation $b\bar{b} \rightarrow A$ is a sizeable contribution to pseudoscalar Higgs production $pp \rightarrow A$. Traditionally, it can be described at NNLO QCD in the five-flavor scheme [65] or at NLO QCD in the four-flavor scheme [66, 67] and theory predictions were based on cross sections matching qualitatively between the two schemes [68]. Since recently theoretically clean matching procedures are also available [69–72], which are numerically very close to the five-flavor scheme. We thus proceed with bottom-quark annihilation described in the five-flavor scheme as implemented in `SusHi 1.6.0`. We compare the gluon-fusion and the bottom-quark annihilation cross sections in the five-flavor scheme for a pseudoscalar of $m_A = 440$ GeV at 13 TeV as a function of $\tan\beta$ in Fig. 1. Around $\tan\beta = 7.5$ both gluon fusion and bottom-quark annihilation are of a similar size, namely 0.3 pb each. For slightly larger values of $\tan\beta$ $b\bar{b} \rightarrow A$ is a bit larger than $gg \rightarrow A$, which appears to be the case for the mild excess in Ref. [31].
- The coupling of the pseudoscalar to Zh is proportional to $\cos(\beta - \alpha)$ which, in the wrong-sign limit, can have values of the order of 0.2 – 0.6. Though the branching ratio $\text{BR}(A \rightarrow Zh)$ will be proportional to the square of this number, the magnitude of it is sufficient to make this the preferred decay channel of A for certain regions of the parameter space, namely those which include the wrong-sign limit. In that case, for intermediate values of $\tan\beta$, the decay mode into Zh also dominates over the decay modes into quark pairs, both $t\bar{t}$ and $b\bar{b}$.

We emphasize that within the Minimal Supersymmetric Standard Model (MSSM) such large values of $\cos(\beta - \alpha)$ are hard to obtain, in particular since in the decoupling limit with $m_A \gg m_Z$ $\cos(\beta - \alpha) \rightarrow 0$ is quickly reached. The alignment limit usually occurs at larger values of $\tan\beta$ [73], if not large values for the soft-breaking parameters or μ are chosen.

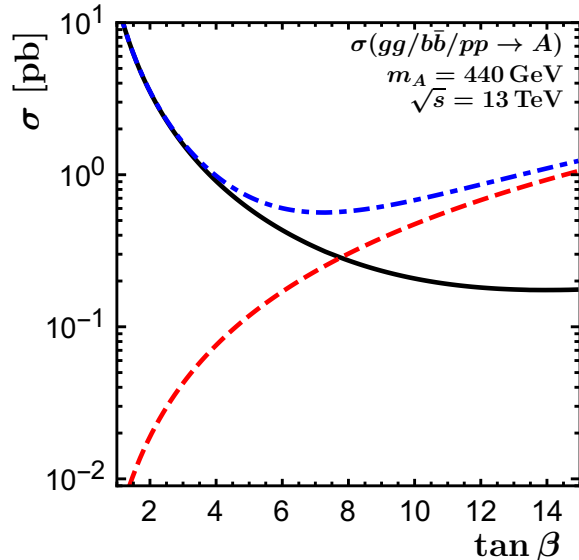


Figure 1: Gluon-fusion cross section (black, solid) and bottom-quark annihilation cross section (red, dashed) and their sum (blue, dot-dashed) for a pseudoscalar with mass 440 GeV at a center-of-mass energy of 13 TeV as a function of $\tan \beta$.

To illustrate the above statements we use a data set generated by `ScannerS` [9, 74–76]. We imposed the tree-level theoretical constraints of boundedness from below [44, 46] and perturbative unitarity [44]. We additionally required the electroweak vacuum to be the global minimum of the tree-level Higgs potential [77]. These constraints were imposed only at the electroweak scale. We did not consider the issue of requiring validity of the model up to higher scales, which would further constrain the theory’s parameter space (see, for instance, Refs. [56, 78, 79]). We checked experimental bounds from B -physics, of which the aforementioned constraint on $b \rightarrow s\gamma$ is the most important one. Electroweak precision measurements were taken into account through bounds on the oblique parameters S , T and U [80]. The branching ratios, decay widths and production cross sections of all Higgs bosons were calculated using `HDECAY 6.511` [81, 82] and `SusHi 1.6.0` [57, 64]². Thus, the bottom-quark annihilation cross section is based on the five-flavor scheme description. This information was passed to `HiggsBounds 4.3.1` [86–89] to check exclusion bounds from searches for additional Higgs bosons. We finally required that the 125 GeV scalar is very much SM-like. We achieve this by demanding that the rates

$$\mu_X = \frac{\sigma^{2\text{HDM}}(pp \rightarrow h) \text{BR}^{2\text{HDM}}(h \rightarrow X)}{\sigma^{\text{SM}}(pp \rightarrow h) \text{BR}^{\text{SM}}(h \rightarrow X)} \quad (8)$$

are within at most 20% of their expected SM values (*i.e.* 1). This ensures a very good compliance with current LHC bounds [4]. As already stated, we allow $-\pi/2 \leq \alpha \leq \pi/2$ and $1 \leq \tan \beta \leq 35$. The masses of the non-SM-like Higgs bosons are constrained to $30 \text{ GeV} \leq$

²For the parameter regions of interest these results were verified with `HIGLU` [83] and `2HDMC` [84], respectively. We refer to Ref. [85] for a comparison of the numerical codes available for the 2HDM.

$m_A \leq 1 \text{ TeV}$, $130 \text{ GeV} \leq m_H \leq 1 \text{ TeV}$ and $480 \text{ GeV} \leq m_{H^\pm} \leq 1 \text{ TeV}$ and the soft \mathbb{Z}_2 breaking parameter to $1 \text{ GeV}^2 \leq m_{12}^2 \leq 5 \times 10^5 \text{ GeV}^2$.

Before we explain the details of our results, we emphasize that for our purposes the usage of the narrow-width approximation is still allowed and interference effects among Higgs bosons and/or the SM background can be neglected: in the 2HDM Ref. [90] pointed out the importance of interference effects in $gg(\rightarrow H) \rightarrow VV$ among the heavy Higgs boson, the light Higgs boson and the SM background. Three reference points include a heavy Higgs mass of 400 GeV, very close to the mass region discussed here. For those points large interference occurs in parameter regions where the signal contribution $gg \rightarrow H \rightarrow VV$ has a cross section below $\sim 10^{-2} \text{ pb}$ for moderate values of $\tan \beta$, i.e. beyond the interesting parameter regions discussed here. The same conclusion can be derived for $b\bar{b}(\rightarrow H) \rightarrow VV$. A similar statement holds for $pp(\rightarrow A) \rightarrow Zh$, for which both $gg \rightarrow A \rightarrow Zh$ and $b\bar{b} \rightarrow A \rightarrow Zh$ including the interferences with the background were discussed in Ref. [91]. A new version of `vh@nnlo` [92] will soon allow to study such interferences, at least at leading order in perturbation theory. Therefore, for all relevant processes in this paper, $gg/b\bar{b} \rightarrow H \rightarrow VV$ and $gg/b\bar{b} \rightarrow A \rightarrow Zh$, we can rely on the narrow-width approximation. This allows to take into account higher-order contributions both in production and decay separately.

We first show the branching ratio of $A \rightarrow Zh$ in Fig. 2 as a function of the pseudoscalar mass m_A and $\tan \beta$. We highlighted, in red, the regions of parameter space corresponding to the wrong-sign limit. It is clear from the figures that in the wrong-sign limit the decay $A \rightarrow Zh$ can indeed become the dominant one, even when the 2HDM parameter space is constrained by the LHC requirement that the lightest \mathcal{CP} -even Higgs boson h is SM-like. Fig. 2 (a) demonstrates that large branching ratios are also obtained above the threshold where the decay into a top-quark pair is kinematically open. Fig. 2 (b) shows that the largest branching ratios are obtained for $\tan \beta$ within 3 to 7. On the one hand, for moderate values of $\tan \beta$ the decay into a top-quark pair is suppressed and the decay into a bottom-quark pair is not yet sufficiently enhanced. The minimum of the sum of the partial decay widths to $t\bar{t}$ and $b\bar{b}$ is at $\tan \beta \sim 7.5$ for $m_A = 440 \text{ GeV}$. On the other hand, the wrong-sign limit can accommodate smaller values of $\cos(\beta - \alpha)$ with increasing $\tan \beta$, which explains why $\text{BR}(A \rightarrow Zh)$ is reduced with increasing $\tan \beta$.

The reduction of $\cos(\beta - \alpha)$ with increasing $\tan \beta$ is also apparent in Fig. 3 (a). The blue points are, as before, those for which the light Higgs boson rates are within 20% of the expected SM values. In contrast to the previous figures the red points correspond to the subset of the blue points for which $400 \leq m_A \leq 500 \text{ GeV}$ and $\sigma(pp \rightarrow A \rightarrow Zh \rightarrow Zb\bar{b}) \geq 0.1 \text{ pb}$. Here we sum up both gluon fusion and bottom-quark annihilation to obtain $\sigma(pp \rightarrow A)$. As explained in Ref. [8], the curved band on the right of the plot corresponds to the wrong-sign limit – and indeed we see all red points lie along this band. Thus we confirm that an excess observed in $pp \rightarrow A \rightarrow Zh$ is associated with larger positive values of $\cos(\beta - \alpha)$ and thus the wrong-sign limit. Finally, Fig. 3 (b) depicts the production cross section $\sigma(pp \rightarrow A)$ in pb as a function of $\tan \beta$, again summing up both gluon fusion and bottom-quark annihilation. Notice how the red points, for which the cross section of $pp \rightarrow A \rightarrow Zh$ is sizeable, seem to follow a descending line up to $\tan \beta \simeq 7.5$, and increase from that point on. This inflexion marks the value of $\tan \beta$ for which the bottom-quark initiated production process becomes as important as gluon fusion, as we illustrated in Fig. 1.

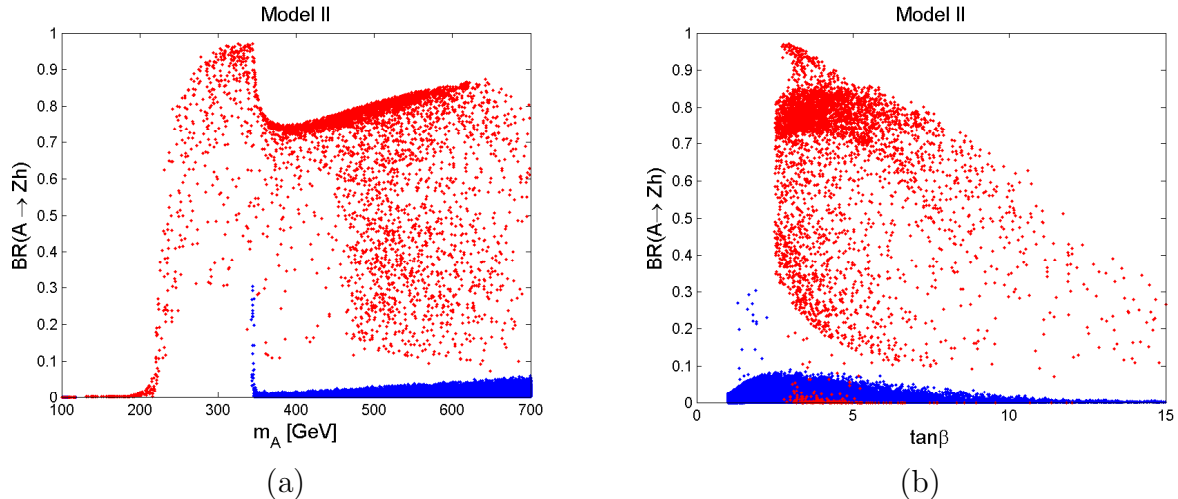


Figure 2: Scatter plots for the 2HDM of type II showing (a) $BR(A \rightarrow Zh)$ as a function of the pseudoscalar mass m_A in GeV and (b) $BR(A \rightarrow Zh)$ as a function of $\tan\beta$. All relevant constraints are imposed and h rates are within 20% of their SM values. Red points are in the wrong-sign limit.

Finally, we split the cross section into gluon fusion and bottom-quark annihilation and combine it with the branching ratios $A \rightarrow Zh$ and $h \rightarrow b\bar{b}$ in Fig. 4 (a) and (b). In those figures we also indicate the measured bounds from the ATLAS analysis [31] as black lines. For the wrong-sign limit we distinguish different regions of $\tan\beta$, namely $1 < \tan\beta < 5$, $5 < \tan\beta < 7.5$ and $\tan\beta > 7.5$ with red, yellow and green points, respectively. It is apparent that in most of the wrong-sign limit parameter space larger cross sections are obtained for the gluon-fusion process, which can be understood from the fact that points with $\tan\beta < 5$ are favoured in our data set, see Fig. 2 (b). Still the wrong-sign limit allows for sufficient room to also have $\sigma(b\bar{b} \rightarrow A)BR(A \rightarrow Zh \rightarrow Zb\bar{b}) > 0.1$ pb at values of $\tan\beta > 5$. Such values of $\tan\beta$ are on the other hand not yet excluded by the gluon-fusion induced process, see Fig. 4 (b). Please note that a much larger cross section observed in the bottom-quark initiated production process is hard to achieve theoretically. Thus if the excess in $\sigma(b\bar{b} \rightarrow A)BR(A \rightarrow Zh \rightarrow Zb\bar{b})$ rises to a significantly larger cross section, the wrong-sign limit of the 2HDM of type II cannot provide an explanation. It is also clear that the investigation of both production processes separately allows for a conclusive probe of the wrong-sign limit of the 2HDM of type II. Ref. [42] shows that at low $\tan\beta$ the process $gg \rightarrow A \rightarrow Zh$ rules out a large parameter region of the wrong-sign limit, see e.g. their Fig. 4. This is in full accordance with our observations, where only values of $\tan\beta > 5$ are not yet excluded by $gg \rightarrow A \rightarrow Zh$.

An interesting feature of the exclusion through the process $pp \rightarrow A \rightarrow Zh \rightarrow Zb\bar{b}$ is the fact that $h \rightarrow b\bar{b}$ vanishes for $\cos(\beta - \alpha) \cdot \tan\beta \approx 1$. As indicated in the caption of Fig. 6 of Ref. [31] this causes a nonexcluded parameter region for low $\tan\beta$ far away from $\cos(\beta - \alpha) = 0$. Obviously, this region can however be excluded through the measurement of the light Higgs boson couplings to bottom quarks and does not correspond to the wrong-sign limit, which occurs at values of $\cos(\beta - \alpha) \tan\beta$ being twice as large.

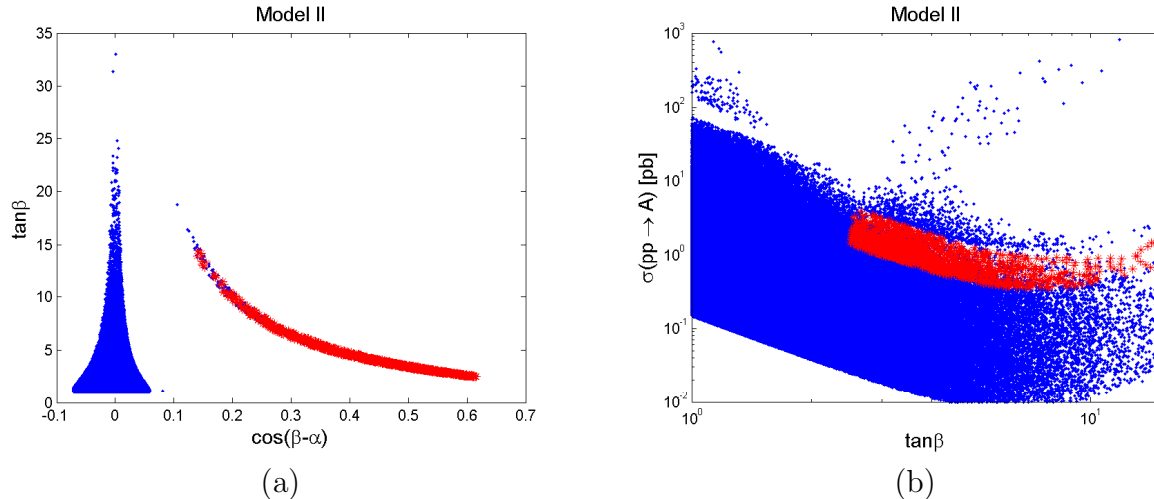


Figure 3: Scatter plots for the 2HDM of type II showing (a) $\tan\beta$ versus $\cos(\beta - \alpha)$ and (b) the cross section for $pp \rightarrow A$ in pb as a function of $\tan\beta$. All relevant constraints are imposed and h rates are within 20% of their SM values. Red points further satisfy $400 \leq m_A \leq 500$ GeV and $\sigma(pp \rightarrow A \rightarrow Zh \rightarrow Zb\bar{b}) \geq 0.1$ pb.

4 Observable consequences of an excess in $pp \rightarrow A \rightarrow Zh$

Since the 2HDM is such a tightly constrained model, having an excess on a particular channel usually has consequences for other ones. In the case we are studying, the region of parameter space which explains an eventual excess in $\sigma(pp \rightarrow A \rightarrow Zh \rightarrow Zb\bar{b})$ is in the wrong-sign limit, the coupling of the lightest Higgs boson to down-type quarks being of an opposite sign to the corresponding SM quantity. Furthermore, the relevant range of $\tan\beta$ values implies that, for the pseudoscalar, the $b\bar{b}$ production mechanism is as important as the gluon-fusion process. We will now show what such an excess would imply for the two other non-SM-like scalars of the theory – H and H^\pm .

We first consider Fig. 5 (a). We show the allowed values of the charged scalar mass m_{H^\pm} and the heavy \mathcal{CP} -even Higgs mass, m_H . Clearly an excess in the channel $pp \rightarrow A \rightarrow Zh \rightarrow Zb\bar{b}$ would require the two remaining scalars to have masses below about 700 GeV – as was to be expected, since the wrong-sign limit cannot occur for very large masses [8]. The lower limit on m_{H^\pm} observed in this figure was imposed from the start, and pertains, as explained above, to bounds on $b \rightarrow s\gamma$. In fact, the most recent results from B -physics calculations [55] already set this lower bound at 580 GeV – which, we observe, could already be in conflict with further constrained points, *i.e.* those for which the lightest \mathcal{CP} -even scalar does not deviate from SM behavior by more than 10%. Nonetheless, if the $pp \rightarrow A \rightarrow Zh \rightarrow Zb\bar{b}$ excess were confirmed, this figure would give us the mass range upon which the remaining 2HDM scalars would have to be found, their masses at most $\sim (150 - 300)$ GeV apart.

As we argued previously the coupling of the heavy \mathcal{CP} -even Higgs boson to two heavy gauge bosons is proportional to $\cos(\beta - \alpha)$, and similarly the decay into two light \mathcal{CP} -even Higgs bosons increases with $\cos(\beta - \alpha)$. It is thus not surprising that such decays are very sensitive to

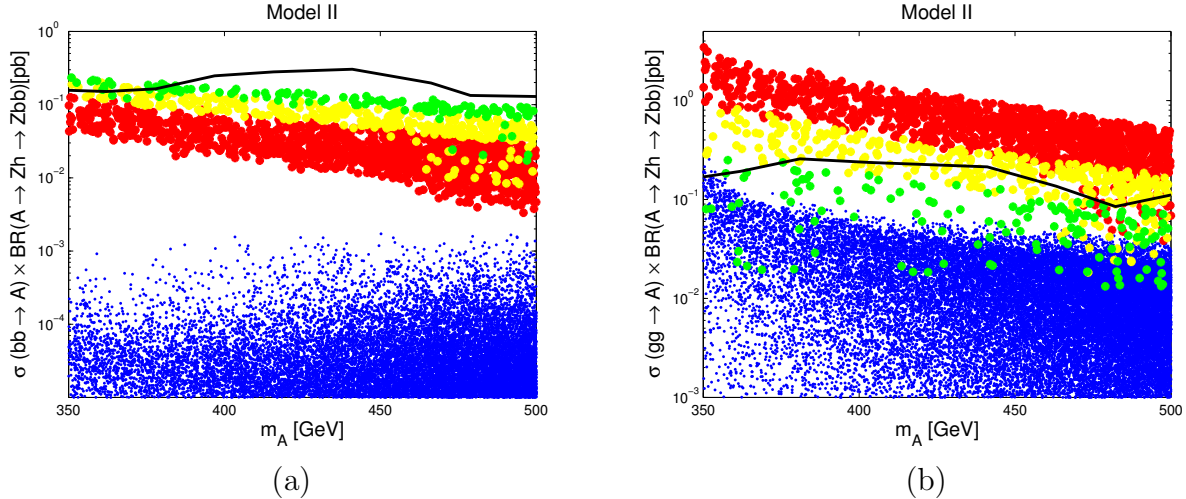


Figure 4: Scatter plots for the 2HDM of type II showing (a) the cross section $\sigma(b\bar{b} \rightarrow A)BR(A \rightarrow Zh \rightarrow Zb\bar{b})$ in pb as a function of m_A in GeV and (b) the cross section $\sigma(gg \rightarrow A)BR(A \rightarrow Zh \rightarrow Zb\bar{b})$ in pb as a function of m_A in GeV. All relevant constraints are imposed and h rates are within 20% of their SM values. Red, yellow and green points represent those parameters satisfying the wrong-sign limit and distinguish different regions of $\tan\beta$: $1 < \tan\beta < 5$ (red), $5 < \tan\beta < 7.5$ (yellow) and $\tan\beta > 7.5$ (green). The black lines indicate the experimental bounds from Ref. [31].

the wrong-sign limit as well. Fig. 5 (b) displays the expected values for the 2HDM cross section for the gluon-induced process $gg \rightarrow H \rightarrow ZZ$. Such searches for heavy Higgs bosons decaying into heavy gauge bosons are currently being probed at the LHC by both the ATLAS [18–22] and CMS [23–25] collaborations. The black line shown in this figure corresponds to the upper $2\text{-}\sigma$ bound from nonobservation of the recent ATLAS analysis [22] – the CMS results would not be significantly different – and therefore gives us an idea where the current experimental sensitivity to this process is. What is clear from the displayed figure is that the points corresponding to the wrong-sign limit lie very closely to the black line. Therefore, the 2HDM explanation for an excess in $pp \rightarrow A \rightarrow Zh$ would imply a signal in the channel $pp \rightarrow H \rightarrow ZZ$ of a magnitude that can surely be probed in the next years. At larger values of $\tan\beta$ the constraints originating from the gluon-induced channel are also weaker. It is worth mentioning that in type II models the coupling of H to bottom quarks is proportional to $\cos\alpha/\cos\beta$. Since SM-like behavior for the light Higgs boson h implies $\beta - \alpha \simeq \pi/2$, this coupling is essentially growing as $\tan\beta$. As such, the $b\bar{b}$ production process for H will have a significant contribution, as it did for A production, and can thus constrain the regions with larger values of $\tan\beta$.

At 13 TeV both ATLAS and CMS collected various constraints on production cross sections of heavy Higgs bosons decaying into a pair of light Higgs bosons at 125 GeV. Those searches include various di-Higgs final states: $b\bar{b}\gamma\gamma$ [34,35], $b\bar{b}b\bar{b}$ [36–38], $W^+W^-\gamma\gamma$ [39], $b\bar{b}W^+W^-/ZZ$ [40] and $b\bar{b}\tau^+\tau^-$ [41]. Still, these searches cannot yet test conclusively the wrong-sign limit: for the parameter space region where the $pp \rightarrow A \rightarrow Zh$ excess occurs, the values for the production cross section of $pp \rightarrow H \rightarrow hh$ are an order of magnitude below the current experimental

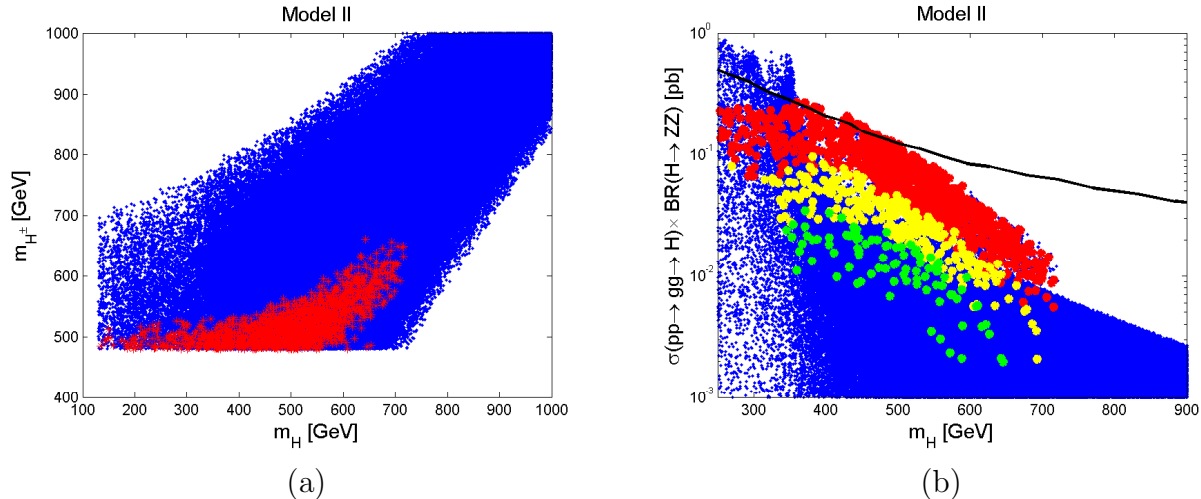


Figure 5: Scatter plots for the 2HDM of type II showing (a) the charged Higgs mass m_{H^\pm} versus the heavier \mathcal{CP} -even Higgs mass m_H , both in GeV, and (b) the gluon-fusion induced cross section for $gg \rightarrow H \rightarrow ZZ$ as a function of m_H in GeV. All relevant constraints are imposed and h rates are within 20% of their SM values. In (a) red points further satisfy $400 \leq m_A \leq 500$ GeV and $\sigma(pp \rightarrow A \rightarrow Zh \rightarrow Zb\bar{b}) \geq 0.1$ pb. In (b) red, yellow and green points are in the wrong-sign limit and distinguish different regions of $\tan \beta$: $1 < \tan \beta < 5$ (red), $5 < \tan \beta < 7.5$ (yellow) and $\tan \beta > 7.5$ (green). The black line in (b) corresponds to the upper $2 - \sigma$ bound from the ATLAS analysis [22] based on an integrated luminosity of 36fb^{-1} .

bounds, so we refrain from showing the corresponding figures.

Finally, let us remember that the wrong-sign limit is a nondecoupling regime. There are “irreducible” contributions to the gluon-fusion cross section and the di-photon decay width which make it so that the light Higgs boson h can never have production and decay rates *exactly* like those of the SM Higgs. For the di-photon width, this stems from a destructive contribution to the amplitude from the charged scalar, essentially independent of m_{H^\pm} for masses up to ~ 700 GeV, see Ref. [8]. As such the wrong-sign limit can be ruled out if measurements of sufficient precision are performed on the lightest Higgs rates. To illustrate this, consider Fig. 6, where we present the signal strength $\mu_{\gamma\gamma}$ versus μ_{ZZ} for the lightest Higgs boson.

The lower band of points in this figure corresponds to the wrong-sign limit, and it is clear it does not include the point (1,1) corresponding to the SM expected values. Further, we see that the yellow points, corresponding to an excess in $\sigma(pp \rightarrow A \rightarrow Zh \rightarrow Zb\bar{b})$ of at least 0.1 pb and SM-like signal strengths within 10%, would imply a di-photon rate for h at least 5% *smaller* than its SM expectation, and a ZZ rate at least 7% *larger* than the SM value. Similar enhancements are predicted for the WW , $\tau\bar{\tau}$ and $b\bar{b}$ channels, all of them arising from a positive interference in the wrong-sign limit between the top and bottom quark contributions to the gluon-fusion cross section³.

³Please notice that the amount of enhancement of the gluon-fusion cross section in the wrong-sign limit is lowered by the inclusion of higher-order QCD corrections with respect to the LO cross section [8], as observed for the reduction of the cross section in the SM case.

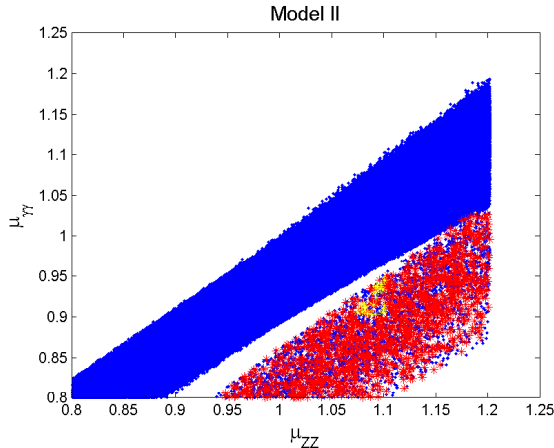


Figure 6: Di-photon decay rate $\mu_{\gamma\gamma}$ versus ZZ production and decay rate μ_{ZZ} for the lightest \mathcal{CP} -even Higgs boson in the 2HDM of type II. It applies the same colour code as in Fig. 3, highlighting in yellow points where the rates of the lightest \mathcal{CP} -even Higgs-boson deviate from the SM values by at most 10%.

5 Conclusions

We conclude that the wrong-sign limit in the 2HDM of type II leads to enhanced and often dominant branching ratios of $A \rightarrow Zh$ and $H \rightarrow VV$, due to sizeable values of $\cos(\beta - \alpha)$. It is thus possible to produce an excess in the current searches of heavy Higgs bosons decaying into Higgs and/or gauge bosons at the LHC. We demonstrated this enhancement for $pp \rightarrow Zb\bar{b}$, stemming from the production of a pseudoscalar A with mass above the $t\bar{t}$ threshold and its subsequent decay to Zh , the SM-like Higgs then decaying further to a pair of bottom quarks. This statement applies to moderate values of $\tan\beta$ – below 15, above roughly 3 – which are experimentally not yet excluded by searches for heavy Higgs bosons decaying into fermions. At intermediate values of $\tan\beta$ between ~ 5 and ~ 7.5 the signal in the bottom-quark induced process is likely to be accompanied by a signal in the gluon-fusion process. The wrong-sign limit makes testable predictions also for the lightest \mathcal{CP} -even Higgs boson couplings, namely enhancing the gluon fusion cross section and lowering the decay rate into two photons. The mild excess currently seen by the ATLAS collaboration in $pp \rightarrow Zb\bar{b}$ is entirely in agreement with the current precision achieved for the couplings of the lightest Higgs boson.

Acknowledgements

This work began during the *Higgs Days at Santander – 2017* workshop. We thank Sven Heinemeyer for financial support and providing a rich discussion environment and Hotel Chiqui for a renovated lobby with decent couches. S.L. acknowledges support from "BMBF Verbundforschung Teilchenphysik" under grant number 05H15VKCCA. J.W. acknowledges financial support by the PIER Helmholtz Graduate School.

References

- [1] **ATLAS** Collaboration, G. Aad *et al.*, *Observation of a new particle in the search for the Standard Model Higgs boson with the ATLAS detector at the LHC*. Phys. Lett. **B716** (2012) 1–29, [arXiv:1207.7214 \[hep-ex\]](#).
- [2] **CMS** Collaboration, S. Chatrchyan *et al.*, *Observation of a new boson at a mass of 125 GeV with the CMS experiment at the LHC*. Phys. Lett. **B716** (2012) 30–61, [arXiv:1207.7235 \[hep-ex\]](#).
- [3] **ATLAS, CMS** Collaboration, G. Aad *et al.*, *Combined Measurement of the Higgs Boson Mass in pp Collisions at $\sqrt{s} = 7$ and 8 TeV with the ATLAS and CMS Experiments*. Phys. Rev. Lett. **114** (2015) 191803, [arXiv:1503.07589 \[hep-ex\]](#).
- [4] **ATLAS, CMS** Collaboration, G. Aad *et al.*, *Measurements of the Higgs boson production and decay rates and constraints on its couplings from a combined ATLAS and CMS analysis of the LHC pp collision data at $\sqrt{s} = 7$ and 8 TeV*. JHEP **08** (2016) 045, [arXiv:1606.02266 \[hep-ex\]](#).
- [5] T. D. Lee, *A Theory of Spontaneous T Violation*. Phys. Rev. **D8** (1973) 1226–1239.
- [6] S. L. Glashow and S. Weinberg, *Natural Conservation Laws for Neutral Currents*. Phys. Rev. **D15** (1977) 1958.
- [7] E. A. Paschos, *Diagonal Neutral Currents*. Phys. Rev. **D15** (1977) 1966.
- [8] P. M. Ferreira, J. F. Gunion, H. E. Haber, and R. Santos, *Probing wrong-sign Yukawa couplings at the LHC and a future linear collider*. Phys. Rev. **D89** (2014) no. 11, 115003, [arXiv:1403.4736 \[hep-ph\]](#).
- [9] P. M. Ferreira, R. Guedes, M. O. P. Sampaio, and R. Santos, *Wrong sign and symmetric limits and non-decoupling in 2HDMs*. JHEP **12** (2014) 067, [arXiv:1409.6723 \[hep-ph\]](#).
- [10] B. Dumont, J. F. Gunion, Y. Jiang, and S. Kraml, *Constraints on and future prospects for Two-Higgs-Doublet Models in light of the LHC Higgs signal*. Phys. Rev. **D90** (2014) 035021, [arXiv:1405.3584 \[hep-ph\]](#).
- [11] D. Fontes, J. C. Romão, and J. P. Silva, *A reappraisal of the wrong-sign $h\bar{b}b$ coupling and the study of $h \rightarrow Z\gamma$* . Phys. Rev. **D90** (2014) no. 1, 015021, [arXiv:1406.6080 \[hep-ph\]](#).
- [12] J. Bernon, J. F. Gunion, Y. Jiang, and S. Kraml, *Light Higgs bosons in Two-Higgs-Doublet Models*. Phys. Rev. **D91** (2015) no. 7, 075019, [arXiv:1412.3385 \[hep-ph\]](#).
- [13] A. Biswas and A. Lahiri, *Alignment, reverse alignment, and wrong sign Yukawa couplings in two Higgs doublet models*. Phys. Rev. **D93** (2016) no. 11, 115017, [arXiv:1511.07159 \[hep-ph\]](#).
- [14] T. Modak, J. C. Romão, S. Sadhukhan, J. a. P. Silva, and R. Srivastava, *Constraining wrong-sign $h\bar{b}b$ couplings with $h \rightarrow \Upsilon\gamma$* . Phys. Rev. **D94** (2016) no. 7, 075017, [arXiv:1607.07876 \[hep-ph\]](#).
- [15] **ATLAS** Collaboration, M. Aaboud *et al.*, *Search for additional heavy neutral Higgs and gauge bosons in the ditau final state produced in 36 fb^{-1} of pp collisions at $\sqrt{s} = 13 \text{ TeV}$ with the ATLAS detector*. [arXiv:1709.07242 \[hep-ex\]](#).
- [16] **CMS** Collaboration, *Search for a neutral MSSM Higgs boson decaying into $\tau\tau$ with 12.9 fb^{-1} of data at $\sqrt{s} = 13 \text{ TeV}$* . Tech. Rep. CMS-PAS-HIG-16-037, CERN, Geneva, 2016. <http://cds.cern.ch/record/2231507>.
- [17] **ATLAS** Collaboration, M. Aaboud *et al.*, *Search for heavy Higgs bosons A/H decaying to a top quark pair in pp collisions at $\sqrt{s} = 8 \text{ TeV}$ with the ATLAS detector*. [arXiv:1707.06025 \[hep-ex\]](#).
- [18] **ATLAS** Collaboration, M. Aaboud *et al.*, *Search for WW/WZ resonance production in $\ell\nu q\bar{q}$ final states in pp collisions at $\sqrt{s} = 13 \text{ TeV}$ with the ATLAS detector*. [arXiv:1710.07235 \[hep-ex\]](#).

- [19] **ATLAS** Collaboration, M. Aaboud *et al.*, *Searches for heavy ZZ and ZW resonances in the $\ell\ell q\bar{q}$ and $\nu\nu q\bar{q}$ final states in pp collisions at $\sqrt{s} = 13$ TeV with the ATLAS detector*. arXiv:1708.09638 [hep-ex].
- [20] **ATLAS** Collaboration, M. Aaboud *et al.*, *Search for heavy resonances decaying into WW in the $e\nu\mu\nu$ final state in pp collisions at $\sqrt{s} = 13$ TeV with the ATLAS detector*. arXiv:1710.01123 [hep-ex].
- [21] **ATLAS** Collaboration, *Study of the Higgs boson properties and search for high-mass scalar resonances in the $H \rightarrow ZZ^* \rightarrow 4\ell$ decay channel at $\sqrt{s} = 13$ TeV with the ATLAS detector* Tech. Rep. ATLAS-CONF-2016-079, CERN, Geneva, Aug, 2016. <http://cds.cern.ch/record/2206253>.
- [22] **ATLAS** Collaboration, *Search for heavy ZZ resonances in the $\ell^+\ell^-\ell^+\ell^-$ and $\ell^+\ell^-\nu\bar{\nu}$ final states using proton-proton collisions at $\sqrt{s} = 13$ TeV with the ATLAS detector* Tech. Rep. ATLAS-CONF-2017-058, CERN, Geneva, Jul, 2017. <http://cds.cern.ch/record/2273874>.
- [23] **CMS** Collaboration, *Search for a heavy scalar boson decaying into a pair of Z bosons in the $2\ell 2\nu$ final state* Tech. Rep. CMS-PAS-HIG-16-001, CERN, Geneva, 2016. <https://cds.cern.ch/record/2140099>.
- [24] **CMS** Collaboration, *Measurements of properties of the Higgs boson and search for an additional resonance in the four-lepton final state at $\sqrt{s} = 13$ TeV* Tech. Rep. CMS-PAS-HIG-16-033, CERN, Geneva, 2016. <https://cds.cern.ch/record/2204926>.
- [25] **CMS** Collaboration, *Search for new diboson resonances in the dilepton + jets final state at $\sqrt{s} = 13$ TeV with 2016 data* Tech. Rep. CMS-PAS-HIG-16-034, CERN, Geneva, 2017. <https://cds.cern.ch/record/2243295>.
- [26] **ATLAS** Collaboration, M. Aaboud *et al.*, *Search for new phenomena in high-mass diphoton final states using 37 fb^{-1} of proton-proton collisions collected at $\sqrt{s} = 13$ TeV with the ATLAS detector*. Submitted to: Phys. Lett. (2017), arXiv:1707.04147 [hep-ex].
- [27] **CMS** Collaboration, V. Khachatryan *et al.*, *Search for high-mass diphoton resonances in proton-proton collisions at 13 TeV and combination with 8 TeV search*. Phys. Lett. **B767** (2017) 147–170, arXiv:1609.02507 [hep-ex].
- [28] **CMS** Collaboration, V. Khachatryan *et al.*, *Search for a pseudoscalar boson decaying into a Z boson and the 125 GeV Higgs boson in $l^+l^-b\bar{b}$ final states*. Phys. Lett. **B748** (2015) 221–243, arXiv:1504.04710 [hep-ex].
- [29] **ATLAS** Collaboration, G. Aad *et al.*, *Search for a CP-odd Higgs boson decaying to Zh in pp collisions at $\sqrt{s} = 8$ TeV with the ATLAS detector*. Phys. Lett. **B744** (2015) 163–183, arXiv:1502.04478 [hep-ex].
- [30] **ATLAS** Collaboration, *Search for a CP-odd Higgs boson decaying to Zh in pp collisions at $\sqrt{s} = 13$ TeV with the ATLAS detector* Tech. Rep. ATLAS-CONF-2016-015, CERN, Geneva, Mar, 2016. <http://cds.cern.ch/record/2141003>.
- [31] **ATLAS** Collaboration, *Search for heavy resonances decaying to a W or Z boson and a Higgs boson in final states with leptons and b-jets in 36.1 fb^{-1} of pp collision data at $\sqrt{s} = 13$ TeV with the ATLAS detector* Tech. Rep. ATLAS-CONF-2017-055, CERN, Geneva, Jul, 2017. <http://cds.cern.ch/record/2273871>.
- [32] **CMS** Collaboration, V. Khachatryan *et al.*, *Search for neutral resonances decaying into a Z boson and a pair of b jets or τ leptons*. Phys. Lett. **B759** (2016) 369–394, arXiv:1603.02991 [hep-ex].
- [33] **CMS** Collaboration, *Search for H to Z(ll)+A($b\bar{b}$) with 2015 data* Tech. Rep. CMS-PAS-HIG-16-010, CERN, Geneva, 2016. <http://cds.cern.ch/record/2140613>.
- [34] **ATLAS** Collaboration, *Search for Higgs boson pair production in the $b\bar{b}\gamma\gamma$ final state using pp collision data at $\sqrt{s} = 13$ TeV with the ATLAS detector* Tech. Rep. ATLAS-CONF-2016-004, CERN, Geneva, Mar, 2016. <http://cds.cern.ch/record/2138949>.

- [35] **CMS** Collaboration, *Search for Higgs boson pair production in the final state containing two photons and two bottom quarks in proton-proton collisions at $\sqrt{s} = 13$ TeV* Tech. Rep. CMS-PAS-HIG-17-008, CERN, Geneva, 2017. <https://cds.cern.ch/record/2273383>.
- [36] **ATLAS** Collaboration, M. Aaboud *et al.*, *Search for pair production of Higgs bosons in the $b\bar{b}b\bar{b}$ final state using proton-proton collisions at $\sqrt{s} = 13$ TeV with the ATLAS detector*. Phys. Rev. **D94** (2016) no. 5, 052002, [arXiv:1606.04782](https://arxiv.org/abs/1606.04782) [hep-ex].
- [37] **CMS** Collaboration, *Search for heavy resonances decaying to a pair of Higgs bosons in the four b quark final state in proton-proton collisions at $\sqrt{s} = 13$ TeV* Tech. Rep. CMS-PAS-B2G-16-026, CERN, Geneva, 2017. <https://cds.cern.ch/record/2264684>.
- [38] **ATLAS** Collaboration, *Search for pair production of Higgs bosons in the $b\bar{b}b\bar{b}$ final state using proton-proton collisions at $\sqrt{s} = 13$ TeV with the ATLAS detector* Tech. Rep. ATLAS-CONF-2016-049, CERN, Geneva, Aug, 2016. <http://cds.cern.ch/record/2206131>.
- [39] **ATLAS** Collaboration, *Search for Higgs boson pair production in the final state of $\gamma\gamma WW^* (\rightarrow lvjj)$ using 13.3 fb^{-1} of pp collision data recorded at $\sqrt{s} = 13$ TeV with the ATLAS detector* Tech. Rep. ATLAS-CONF-2016-071, CERN, Geneva, Aug, 2016. <http://cds.cern.ch/record/2206222>.
- [40] **CMS** Collaboration, A. M. Sirunyan *et al.*, *Search for resonant and nonresonant Higgs boson pair production in the $b\bar{b}l\nu l\nu$ final state in proton-proton collisions at $\sqrt{s} = 13$ TeV*. [arXiv:1708.04188](https://arxiv.org/abs/1708.04188) [hep-ex].
- [41] **CMS** Collaboration, A. M. Sirunyan *et al.*, *Search for Higgs boson pair production in events with two bottom quarks and two tau leptons in proton-proton collisions at $\sqrt{s} = 13$ TeV*. [arXiv:1707.02909](https://arxiv.org/abs/1707.02909) [hep-ex].
- [42] L. Wang, F. Zhang, and X.-F. Han, *Two-Higgs-doublet model of type-II confronted with the LHC run-I and run-II data*. Phys. Rev. **D95** (2017) no. 11, 115014, [arXiv:1701.02678](https://arxiv.org/abs/1701.02678) [hep-ph].
- [43] **ATLAS** Collaboration, M. Aaboud *et al.*, *Search for heavy resonances decaying to a W or Z boson and a Higgs boson in the $q\bar{q}^{(\prime)}b\bar{b}$ final state in pp collisions at $\sqrt{s} = 13$ TeV with the ATLAS detector*. Phys. Lett. **B774** (2017) 494–515, [arXiv:1707.06958](https://arxiv.org/abs/1707.06958) [hep-ex].
- [44] G. C. Branco, P. M. Ferreira, L. Lavoura, M. N. Rebelo, M. Sher, and J. P. Silva, *Theory and phenomenology of two-Higgs-doublet models*. Phys. Rept. **516** (2012) 1–102, [arXiv:1106.0034](https://arxiv.org/abs/1106.0034) [hep-ph].
- [45] N. G. Deshpande and E. Ma, *Pattern of Symmetry Breaking with Two Higgs Doublets*. Phys. Rev. **D18** (1978) 2574.
- [46] K. G. Klimenko, *On Necessary and Sufficient Conditions for Some Higgs Potentials to Be Bounded From Below*. Theor. Math. Phys. **62** (1985) 58–65. [Teor. Mat. Fiz.62,87(1985)].
- [47] I. P. Ivanov, *Minkowski space structure of the Higgs potential in 2HDM*. Phys. Rev. **D75** (2007) 035001, [arXiv:hep-ph/0609018](https://arxiv.org/abs/hep-ph/0609018) [hep-ph]. [Erratum: Phys. Rev. **D76**, 039902 (2007)].
- [48] I. P. Ivanov, *Minkowski space structure of the Higgs potential in 2HDM. II. Minima, symmetries, and topology*. Phys. Rev. **D77** (2008) 015017, [arXiv:0710.3490](https://arxiv.org/abs/0710.3490) [hep-ph].
- [49] S. Kanemura, T. Kubota, and E. Takasugi, *Lee-Quigg-Thacker bounds for Higgs boson masses in a two doublet model*. Phys. Lett. **B313** (1993) 155–160, [arXiv:hep-ph/9303263](https://arxiv.org/abs/hep-ph/9303263) [hep-ph].
- [50] A. G. Akeroyd, A. Arhrib, and E.-M. Naimi, *Note on tree level unitarity in the general two Higgs doublet model*. Phys. Lett. **B490** (2000) 119–124, [arXiv:hep-ph/0006035](https://arxiv.org/abs/hep-ph/0006035) [hep-ph].
- [51] O. Deschamps, S. Descotes-Genon, S. Monteil, V. Niess, S. T’Jampens, and V. Tisserand, *The Two Higgs Doublet of Type II facing flavour physics data*. Phys. Rev. **D82** (2010) 073012, [arXiv:0907.5135](https://arxiv.org/abs/0907.5135) [hep-ph].

- [52] F. Mahmoudi and O. Stål, *Flavor constraints on the two-Higgs-doublet model with general Yukawa couplings*. Phys. Rev. **D81** (2010) 035016, [arXiv:0907.1791 \[hep-ph\]](#).
- [53] T. Hermann, M. Misiak, and M. Steinhauser, $\bar{B} \rightarrow X_s \gamma$ in the Two Higgs Doublet Model up to Next-to-Next-to-Leading Order in QCD. JHEP **11** (2012) 036, [arXiv:1208.2788 \[hep-ph\]](#).
- [54] M. Misiak *et al.*, *Updated NNLO QCD predictions for the weak radiative B-meson decays*. Phys. Rev. Lett. **114** (2015) no. 22, 221801, [arXiv:1503.01789 \[hep-ph\]](#).
- [55] M. Misiak and M. Steinhauser, *Weak Radiative Decays of the B Meson and Bounds on M_{H^\pm} in the Two-Higgs-Doublet Model*. Eur. Phys. J. **C77** (2017) no. 3, 201, [arXiv:1702.04571 \[hep-ph\]](#).
- [56] P. Basler, P. M. Ferreira, M. Mühlleitner, and R. Santos, *High scale impact in alignment and decoupling in two-Higgs doublet models*. [arXiv:1710.10410 \[hep-ph\]](#).
- [57] R. V. Harlander, S. Liebler, and H. Mantler, *SusHi: A program for the calculation of Higgs production in gluon fusion and bottom-quark annihilation in the Standard Model and the MSSM*. Comput. Phys. Commun. **184** (2013) 1605–1617, [arXiv:1212.3249 \[hep-ph\]](#).
- [58] R. V. Harlander and W. B. Kilgore, *Next-to-next-to-leading order Higgs production at hadron colliders*. Phys. Rev. Lett. **88** (2002) 201801, [arXiv:hep-ph/0201206 \[hep-ph\]](#).
- [59] C. Anastasiou and K. Melnikov, *Higgs boson production at hadron colliders in NNLO QCD*. Nucl. Phys. **B646** (2002) 220–256, [arXiv:hep-ph/0207004 \[hep-ph\]](#).
- [60] V. Ravindran, J. Smith, and W. L. van Neerven, *NNLO corrections to the total cross-section for Higgs boson production in hadron hadron collisions*. Nucl. Phys. **B665** (2003) 325–366, [arXiv:hep-ph/0302135 \[hep-ph\]](#).
- [61] R. V. Harlander and W. B. Kilgore, *Production of a pseudoscalar Higgs boson at hadron colliders at next-to-next-to leading order*. JHEP **10** (2002) 017, [arXiv:hep-ph/0208096 \[hep-ph\]](#).
- [62] C. Anastasiou and K. Melnikov, *Pseudoscalar Higgs boson production at hadron colliders in NNLO QCD*. Phys. Rev. **D67** (2003) 037501, [arXiv:hep-ph/0208115 \[hep-ph\]](#).
- [63] M. Spira, A. Djouadi, D. Graudenz, and P. M. Zerwas, *Higgs boson production at the LHC*. Nucl. Phys. **B453** (1995) 17–82, [arXiv:hep-ph/9504378 \[hep-ph\]](#).
- [64] R. V. Harlander, S. Liebler, and H. Mantler, *SusHi Bento: Beyond NNLO and the heavy-top limit*. Comput. Phys. Commun. **212** (2017) 239–257, [arXiv:1605.03190 \[hep-ph\]](#).
- [65] R. V. Harlander and W. B. Kilgore, *Higgs boson production in bottom quark fusion at next-to-next-to leading order*. Phys. Rev. **D68** (2003) 013001, [arXiv:hep-ph/0304035 \[hep-ph\]](#).
- [66] S. Dittmaier, M. Krämer, and M. Spira, *Higgs radiation off bottom quarks at the Tevatron and the CERN LHC*. Phys. Rev. **D70** (2004) 074010, [arXiv:hep-ph/0309204 \[hep-ph\]](#).
- [67] S. Dawson, C. B. Jackson, L. Reina, and D. Wackerroth, *Exclusive Higgs boson production with bottom quarks at hadron colliders*. Phys. Rev. **D69** (2004) 074027, [arXiv:hep-ph/0311067 \[hep-ph\]](#).
- [68] R. Harlander, M. Krämer, and M. Schumacher, *Bottom-quark associated Higgs-boson production: reconciling the four- and five-flavour scheme approach*. [arXiv:1112.3478 \[hep-ph\]](#).
- [69] M. Bonvini, A. S. Papanastasiou, and F. J. Tackmann, *Resummation and matching of b-quark mass effects in $b\bar{b}H$ production*. JHEP **11** (2015) 196, [arXiv:1508.03288 \[hep-ph\]](#).
- [70] M. Bonvini, A. S. Papanastasiou, and F. J. Tackmann, *Matched predictions for the $b\bar{b}H$ cross section at the 13 TeV LHC*. JHEP **10** (2016) 053, [arXiv:1605.01733 \[hep-ph\]](#).
- [71] S. Forte, D. Napoletano, and M. Ubiali, *Higgs production in bottom-quark fusion in a matched scheme*. Phys. Lett. **B751** (2015) 331–337, [arXiv:1508.01529 \[hep-ph\]](#).

- [72] S. Forte, D. Napoletano, and M. Ubiali, *Higgs production in bottom-quark fusion: matching beyond leading order*. Phys. Lett. **B763** (2016) 190–196, [arXiv:1607.00389 \[hep-ph\]](#).
- [73] M. Carena, I. Low, N. R. Shah, and C. E. M. Wagner, *Impersonating the Standard Model Higgs Boson: Alignment without Decoupling*. JHEP **04** (2014) 015, [arXiv:1310.2248 \[hep-ph\]](#).
- [74] R. Coimbra, M. O. P. Sampaio, and R. Santos, *ScannerS: Constraining the phase diagram of a complex scalar singlet at the LHC*. Eur. Phys. J. **C73** (2013) 2428, [arXiv:1301.2599 \[hep-ph\]](#).
- [75] R. Costa, M. Mühlleitner, M. O. P. Sampaio, and R. Santos, *Singlet Extensions of the Standard Model at LHC Run 2: Benchmarks and Comparison with the NMSSM*. JHEP **06** (2016) 034, [arXiv:1512.05355 \[hep-ph\]](#).
- [76] M. Mühlleitner, M. O. P. Sampaio, R. Santos, and J. Wittbrodt, *The N2HDM under Theoretical and Experimental Scrutiny*. JHEP **03** (2017) 094, [arXiv:1612.01309 \[hep-ph\]](#).
- [77] A. Barroso, P. M. Ferreira, I. P. Ivanov, and R. Santos, *Metastability bounds on the two Higgs doublet model*. JHEP **06** (2013) 045, [arXiv:1303.5098 \[hep-ph\]](#).
- [78] N. Chakrabarty, U. K. Dey, and B. Mukhopadhyaya, *High-scale validity of a two-Higgs doublet scenario: a study including LHC data*. JHEP **12** (2014) 166, [arXiv:1407.2145 \[hep-ph\]](#).
- [79] N. Chakrabarty and B. Mukhopadhyaya, *High-scale validity of a two Higgs doublet scenario: predicting collider signals*. Phys. Rev. **D96** (2017) no. 3, 035028, [arXiv:1702.08268 \[hep-ph\]](#).
- [80] **Gfitter Group** Collaboration, M. Baak, J. Cúth, J. Haller, A. Hoecker, R. Kogler, K. Mönig, M. Schott, and J. Stelzer, *The global electroweak fit at NNLO and prospects for the LHC and ILC*. Eur. Phys. J. **C74** (2014) 3046, [arXiv:1407.3792 \[hep-ph\]](#).
- [81] A. Djouadi, J. Kalinowski, and M. Spira, *HDECAY: A Program for Higgs boson decays in the standard model and its supersymmetric extension*. Comput. Phys. Commun. **108** (1998) 56–74, [arXiv:hep-ph/9704448 \[hep-ph\]](#).
- [82] J. M. Butterworth *et al.*, “THE TOOLS AND MONTE CARLO WG Summary Report from the Les Houches 2009 Workshop on TeV Colliders,” in *Physics at TeV colliders. Proceedings, 6th Workshop, dedicated to Thomas Binoth, Les Houches, France, June 8-26, 2009*. [arXiv:1003.1643 \[hep-ph\]](#).
- [83] M. Spira, *HIGLU: A program for the calculation of the total Higgs production cross-section at hadron colliders via gluon fusion including QCD corrections*. [arXiv:hep-ph/9510347 \[hep-ph\]](#).
- [84] D. Eriksson, J. Rathsmann, and O. Stål, *2HDMC: Two-Higgs-Doublet Model Calculator Physics and Manual*. Comput. Phys. Commun. **181** (2010) 189–205, [arXiv:0902.0851 \[hep-ph\]](#).
- [85] R. Harlander, M. Mühlleitner, J. Rathsmann, M. Spira, and O. Stål, *Interim recommendations for the evaluation of Higgs production cross sections and branching ratios at the LHC in the Two-Higgs-Doublet Model*. [arXiv:1312.5571 \[hep-ph\]](#).
- [86] P. Bechtle, O. Brein, S. Heinemeyer, G. Weiglein, and K. E. Williams, *HiggsBounds: Confronting Arbitrary Higgs Sectors with Exclusion Bounds from LEP and the Tevatron*. Comput. Phys. Commun. **181** (2010) 138–167, [arXiv:0811.4169 \[hep-ph\]](#).
- [87] P. Bechtle, O. Brein, S. Heinemeyer, G. Weiglein, and K. E. Williams, *HiggsBounds 2.0.0: Confronting Neutral and Charged Higgs Sector Predictions with Exclusion Bounds from LEP and the Tevatron*. Comput. Phys. Commun. **182** (2011) 2605–2631, [arXiv:1102.1898 \[hep-ph\]](#).
- [88] P. Bechtle, O. Brein, S. Heinemeyer, O. Stål, T. Stefaniak, G. Weiglein, and K. E. Williams, *HiggsBounds – 4: Improved Tests of Extended Higgs Sectors against Exclusion Bounds from LEP, the Tevatron and the LHC*. Eur. Phys. J. **C74** (2014) no. 3, 2693, [arXiv:1311.0055 \[hep-ph\]](#).

- [89] P. Bechtle, S. Heinemeyer, O. Stål, T. Stefaniak, and G. Weiglein, *Applying Exclusion Likelihoods from LHC Searches to Extended Higgs Sectors*. Eur. Phys. J. **C75** (2015) no. 9, 421, [arXiv:1507.06706](#) [[hep-ph](#)].
- [90] N. Greiner, S. Liebler, and G. Weiglein, *Interference contributions to gluon initiated heavy Higgs production in the Two-Higgs-Doublet Model*. Eur. Phys. J. **C76** (2016) no. 3, 118, [arXiv:1512.07232](#) [[hep-ph](#)].
- [91] R. V. Harlander, S. Liebler, and T. Zirke, *Higgs Strahlung at the Large Hadron Collider in the 2-Higgs-Doublet Model*. JHEP **02** (2014) 023, [arXiv:1307.8122](#) [[hep-ph](#)].
- [92] R. V. Harlander, J. Klappert, S. Liebler, and L. Simon, *vh@nnlo-v2: New physics in Higgs Strahlung*. [arXiv:1802.04817](#) [[hep-ph](#)].